Autofluorescence Lifetimes in Geographic Atrophy in Patients With Age-Related Macular Degeneration

Chantal Dysli, Sebastian Wolf, and Martin S. Zinkernagel

Department of Ophthalmology, Inselspital, Bern University Hospital, University of Bern, Bern, Switzerland

Correspondence: Martin S. Zinkernagel, Bern University Hospital, 3010 Bern, Switzerland; m.zinkernagel@gmail.com.

Submitted: October 11, 2015
Accepted: March 4, 2016

Citation: Dysli C, Wolf S, Zinkernagel MS. Autofluorescence lifetimes in geographic atrophy in patients with age-related macular degeneration. *Invest Ophthalmol Vis Sci*. 2016;57:2479–2487. DOI:10.1167/iovs.15-18381

Purpose. To investigate fluorescence lifetime characteristics in patients with geographic atrophy (GA) in eyes with age-related macular degeneration and to correlate the measurements with clinical data and optical coherence tomography (OCT) findings.

Methods. Patients with GA were imaged with a fluorescence lifetime imaging ophthalmoscope. Retinal autofluorescence lifetimes were measured in a short and a long spectral channel (498–560 nm and 560–720 nm). Mean retinal fluorescence lifetimes were analyzed within GA and the surrounding retina, and data were correlated with best corrected visual acuity and OCT measurements.

Results. Fluorescence lifetime maps of 41 eyes of 41 patients (80 ± 7 years) with GA were analyzed. Mean lifetimes within areas of atrophy were prolonged by 624 ± 276 ps (+152%) in the short spectral channel and 418 ± 186 ps (+83%) in the long spectral channel compared to the surrounding tissue. Autofluorescence lifetime abnormalities in GA occurred with particular patterns, similar to those seen in fundus autofluorescence intensity images. Within the fovea short mean autofluorescence lifetimes were observed, presumably representing macular pigment. Short lifetimes were preserved even in the absence of foveal sparing but were decreased in patients with advanced retinal atrophy in OCT. Short lifetimes in the fovea correlated with better best corrected visual acuity in both spectral channels.

Conclusions. This study established that autofluorescence lifetime changes in GA present with explicit patterns. We hypothesize that the short lifetimes seen within the atrophy may be used to estimate damage induced by atrophy and to monitor disease progression in the context of natural history or interventional therapeutic studies.

Keywords: fundus autofluorescence, fluorescence lifetimes, ophthalmic imaging, GA, geographic atrophy, AMD, age-related macular degeneration

Geographic atrophy (GA) is the end stage of dry age-related macular degeneration (AMD) and is characterized by slow and progressing degeneration of the retinal pigment epithelium, the choriocapillaris, and the outer retina.[1] Advanced dry AMD with GA leads to progressive irreversible loss of central vision and is one of the leading causes for blindness,[2] accounting for up to 20% of severe vision loss in North America.[3] Despite being a thoroughly investigated and clinically well characterized disease, the molecular pathways leading to atrophy in dry AMD are complex and multifactorial. Epidemiologic studies have identified advanced age, smoking, and nutrition as risk factors for the development of GA. Furthermore, certain complement pathway genes including complement component 3 and complement factor H and I have been shown to be risk factors for the development and progression of AMD.[4,5]

Recent advances in retinal imaging technologies have improved the understanding of morphological changes that occur in complex-trait macular diseases such as GA. Fundus autofluorescence (FAF) imaging allows a refined measurement of the GA area, disease progression, and characterization of GA phenotypes.[6,7] Longitudinal observations have shown that the latter has an impact on atrophy and therefore can be used as a prognostic determinant.[8]

The fundus autofluorescence signal is mainly generated by RPE lipofuscin, a mixture of fluorophores originating from byproducts of the visual cycle.[9,10] As a result of RPE loss and the subsequent decrease of lipofuscin that occurs in advanced GA, there is a loss of signal in the FAF. However, in the junctional zone surrounding atrophy, FAF has been shown to be increased. The increased autofluorescence signal could be a result of increased phagocytosis with lipofuscin accumulation or formation of RPE multilayers.[11,12] Alternatively, increased bisretinoid formation within impaired photoreceptors has been proposed to be causative for increased autofluorescence in the junctional zone.[13]

High-resolution optical coherence tomography (OCT) has advanced the study of GA with its unprecedented resolution, and thus it has provided further insights in the disease process and has been reported to be useful to identify areas of foveal sparing.[14] OCT characteristics of GA include choroidal signal enhancement and alterations at the level of RPE, the outer nuclear layer (ONL) and outer plexiform layer (OPL), and the external limiting membrane.

Time-resolved fundus autofluorescence imaging (FLIO) is a relatively novel imaging method that allows topographic mapping of endogenous fluorescence lifetimes within the retina.[15–17] The fluorescence lifetime represents the time a molecule spends in its excited state after excitation with a laser

impulse before returning to its ground state by emission of a photon with a longer wavelength. Autofluorescence lifetimes are specific for each fluorophore and sensitive to the metabolic environment.[18]

The aim of the present study was to characterize autofluorescence lifetimes in GA as a result of AMD and to identify GA phenotypes using FLIO and high-resolution spectral-domain OCT imaging.

Methods

This study is registered at ClinicalTrials.gov (NCT01981148). It was carried out with the approval of the local ethics committee and is in accordance with the International Ethical Guidelines for Biomedical Research involving Human Subjects (Council for International Organizations of Medical Sciences) and the Declaration of Helsinki.

Patients

Patients with GA and AMD were recruited at the Outpatient Department of Ophthalmology at the Bern University Hospital, Bern, Switzerland, and signed an informed consent prior to study entry. None of the patients reported taking carotenoid supplementation.

Patient selection was relayed on the clinical diagnosis that was confirmed by OCT and FAF imaging. Eyes with a history or signs of neovascular AMD and other ophthalmic diseases affecting the macula as well as significant lens opacities were excluded.

Geographic Atrophy

Areas of GA were defined funduscopically with clearly visible marked boundaries of decreased retinal pigmentation and exposed underlying choroidal structures. In FAF, one or more clearly demarked areas of hypoautofluorescence were present, corresponding to areas in OCT with choroidal signal enhancement because of the absence of the retinal pigment epithelium and loss of the external limiting membrane within the fovea. Foveal sparing was defined as a central foveal island with an intact retinal layer structure that was preserved and surrounded by well-demarked areas of GA for at least 270°.

Patient Examinations

For all of the patients included in this study, best corrected visual acuity (BCVA) was assessed (Early Treatment Diabetic Retinopathy Study [ETDRS] letters).[19] Subsequently, pupils were maximally dilated with tropicamid 0.5% and phenylephrine hydrochloride 2.5%, and the fundus was examined biomicroscopically. Color fundus images (Zeiss FF 450plus, Zeiss, Oberkochen, Germany), FAF images, and OCT scans of the macula (Heidelberg Spectralis HRA+OCT; Heidelberg Engineering, Heidelberg, Germany) were obtained. OCT was performed using a high-speed mode and a scan pattern size of 20° × 20° centered on the fovea, resulting in 49 B scans per eye.

Fluorescence lifetime images were acquired using a fluorescence lifetime imaging ophthalmoscope, which is based on an HRA Spectralis system (Heidelberg Engineering).

Fluorescence Lifetime Imaging Ophthalmoscope

The fluorescence lifetime imaging ophthalmoscope uses a 473-nm pulsed blue laser light at an 80-MHz repetition rate for excitation of retinal autofluorescence. Emitted fluorescence light was registered by time-correlated single-photon counting modules using highly sensitive hybrid photon-counting detectors (Becker&Hickl, Berlin, Germany). Two detection channels with distinct wavelengths were used: a short spectral channel (SSC, 498–560 nm) and a long spectral channel (LSC, 560–720 nm). Simultaneously, a confocal high-contrast infrared image was recorded by the system to record each photon at the correct spatial location. A minimal photon count of 1000 photons per pixel was acquired for every location within the image, resulting in a total scan duration of approximately 90 seconds. The Becker&Hickl software (SPCImage 4.6) was used for the analysis of recorded lifetime data, and a biexponential decay model was applied using a binning factor of one. A triexponential fitting procedure, which requires a higher binning factor, did not substantially contribute to a lower χ^2 value, which indicates the goodness of the fit. Therefore, we used a binning of 3 × 3 pixels and two decay components to gain spatial resolution.

This procedure resulted in a short ($T1$) and a long ($T2$) lifetime component with corresponding amplitudes $\alpha 1$ and $\alpha 2$. For each pixel, an intensity-weighted mean fluorescence lifetime value Tm was calculated as follows:

$$Tm = \frac{\alpha 1 * T1 + \alpha 2 * T2}{\alpha 1 + \alpha 2} \quad (1)$$

The basic characteristics of the FLIO device and the analysis method have been further described in previous reports.[15]

Analysis of Fluorescence Lifetime Data

Areas of GA within FAF images were classified according to Bindewald et al.[6] The size of GA was measured manually within FAF images. Fluorescence lifetime data was further analyzed by using the FLIO reader software (ARTORG Center for Biomedical Engineering Research, University of Bern, Bern, Switzerland). A circle of interest with a diameter of 0.2 mm was applied for the quantitative analysis of detailed structures. This circle was placed within predefined areas of a standard early treatment of a diabetic retinopathy (ETDRS) grid with a central area (diameter [d] = 1 mm), an inner ring (d = 3 mm), and an outer ring (d = 6 mm). Image detail sections (d = 0.2 mm) were analyzed within the foveal center and the outer ETDRS ring from the unaffected retina and areas within GA. The image detail section measurements represent a mean value of three individual measurement locations. Fluorescence lifetime data of both spectral channels were analyzed separately. If both eyes showed GA, the eye with the better image quality was chosen.

Analysis of OCT Data

Thickness measurements of retinal layers were performed using a spectral-domain OCT. The inbuilt automated retinal layer segmentation of the Heidelberg software was applied. Total retinal thickness within the foveal center was assessed after manual correction of the automatically segmented inner limiting membrane and the basal membrane. The values were extracted from the central subfield of the ETDRS grid, and a small marker was placed within the foveal center. Choroidal thickness was measured beneath the foveal center.

Statistical Analysis

For statistical analysis, Prism Graph Pad (Prism 6; GraphPad Software, Inc., La Jolla, CA, USA) was used. Within the outer ring of the ETDRS grid, retinal areas within GA were compared with surrounding retinal tissue and with lifetime values from the foveal center. Group comparison was done by one-way ANOVA and Tukey's multiple-comparison posttest analysis

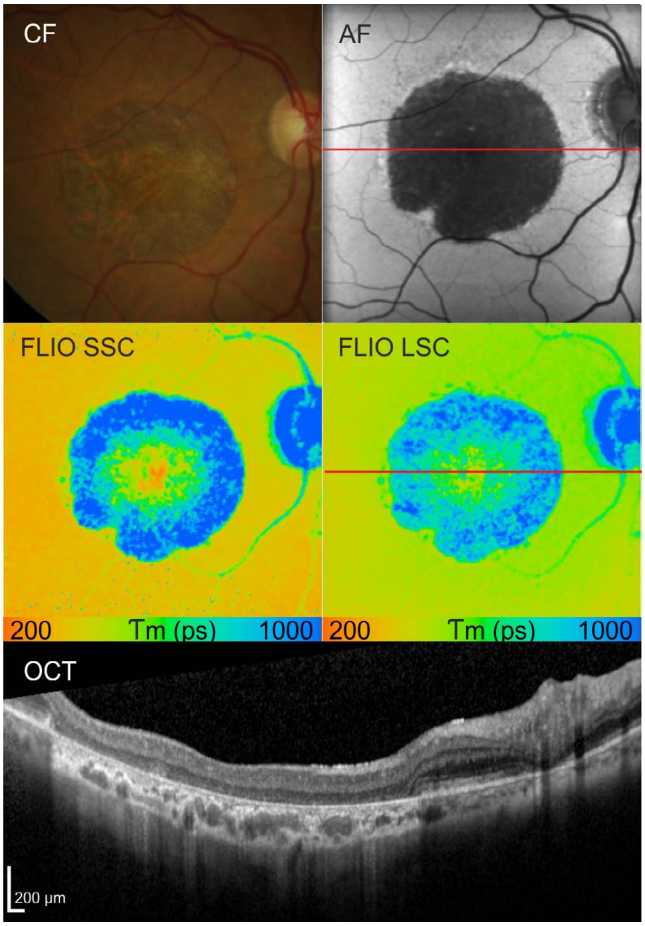

FIGURE 1. Central GA in a patient with dry AMD. CF, color fundus; AF, fundus autofluorescence intensity LSC; FLIO SSC/LSC, mean fluorescence lifetime images of the short and the long spectral channels. OCT scan of the indicated line.

(confidence interval 95%). A linear regression model was used for correlation analysis. *P* values of less than 0.05 were considered to be statistically significant. Multiple linear regression analysis was performed using SigmaPlot Version 12.3 (Systat Software, Inc., San Jose, CA, USA).

RESULTS

A total of 41 eyes with AMD and GA of 41 patients were analyzed (22 right eyes and 19 left eyes). The mean age ± standard deviation of the patients was 80 ± 7 years (range, 66–94) and 54% (22) of the patients were female. Of the investigated eyes, 66% (27 patients) were pseudophacic.

Foveal sparing was seen in 24% (10 patients). The mean area of GA (± standard error of the mean [SEM]) was 14.0 ± 1.8 mm^2 (range, 0.2–50 mm^2). Of the investigated eyes, 34% (14 patients) showed one isolated unifocal lesion, whereas 66% (27 patients) presented with multiple areas of GA. Multifocal lesions were either grouped in main atrophy with satellite lesions (37%, 10 patients) or multiple confluent atrophic areas (63%, 17 patients). According to GA classification of Bindewald et al.,[6] 10% of the eyes (4 patients) showed no increased autofluorescence surrounding GA, 10% (4 patients) presented with focal, 49% (20 patients) with diffuse (reticular, branching, fine granular, trickling, granular with peripheral punctuate spots), 29% (12 patients) with banded, and 2% (1 patient) with patchy hyperfluorescence.

Fluorescence Lifetimes in GA

Representative images of a patient with GA are shown in Figure 1. Areas of decreased autofluorescence intensity in FAF correlated well with the areas of abnormal mean fluorescence lifetime values. Different patterns of GA were associated with specific autofluorescence lifetime patterns (Fig. 2). The mean fluorescence lifetime measured in areas of GA was 1035 ± 52 ps (SEM) in the SSC and 924 ± 36 ps in the LSC (Fig. 3). Therefore, *Tm* was significantly prolonged by 624 ± 276 ps (+152%) in the SSC and 418 ± 186 ps (+83%) in the LSC when compared with the surrounding retinal tissue with mean lifetimes of 411 ± 11 ps and 506 ± 10 ps, respectively ($P < 0.0001$). The coefficient of variation in the SSC was 17% for the retina and 31% within GA, and in the LSC it was 13% in the retina and 24% within GA. Within GA, the mean autofluorescence lifetime of the foveal center was shorter when compared with the surrounding atrophic area (Figs. 1–4), irrespective of foveal sparing (Fig. 5). In seven eyes with progressed atrophy of the outer retinal layers in OCT, the mean fluorescence lifetime distribution did not show a peak of short lifetimes within the macular center but, rather, a speckled pattern (Figs. 6A, 6B).

Fluorescence Lifetimes in Pseudophakic Versus Phakic Patients

In the SSC, the mean fluorescence lifetime values were significantly dependent on the lens status ($P = 0.05$ in the foveal center, <0.001 in the normal retina, and 0.003 in GA areas; multiple linear regression analysis). In the LSC, the values were completely independent of the lens status ($P = 0.41$ in the foveal center, 0.4 in the normal retina, and 0.84 in GA areas). However, because fluorescence lifetimes were analyzed and compared within individual eyes, the lens status as a potential confounder was eliminated.

Fluorescence Lifetimes in GA With Foveal Sparing

Patients with GA and foveal sparing ($n = 10$) showed uniformly prolonged mean autofluorescence lifetimes inside the areas of atrophy. Within the foveal center, typical short mean fluorescence lifetimes were observed (SSC: 295 ± 27 ps; LSC: 401 ± 28 ps; Fig. 5). Mean fluorescence lifetimes within the foveal center of patients with central GA did not significantly differ from values from patients with foveal sparing ($P = 0.67$ and 0.31; Fig. 5B).

FLIO and Visual Acuity

The mean visual acuity in the study eyes was 42 ± 3 ETDRS letters (range, 0–84 letters). There was a significant correlation between BCVA and the mean fluorescence lifetime of the central ETDRS subfield in both spectral channels when analyzing the data of all study eyes ($r^2 = 0.19$, $P = 0.004$; Fig. 7). In a subgroup analysis of eyes with foveal sparing ($n = 10$), r^2 was 0.16 and 0.13, respectively ($P = 0.03$ and 0.04).

FLIO and OCT Analysis

Retinal thickness within atrophic areas was clearly reduced in eyes with GA as a result of AMD (143 ± 12 µm; Figs. 1, 4–6). Outer retinal layers, including the RPE, the photoreceptors, and the ONL and OPL were significantly thinned or completely missing. The RPE showed drusenoid deposits and irregularities that appeared as highly hyper-reflective in the OCT scans. Mean subfoveal choroidal thickness was 139 ± 11 µm.

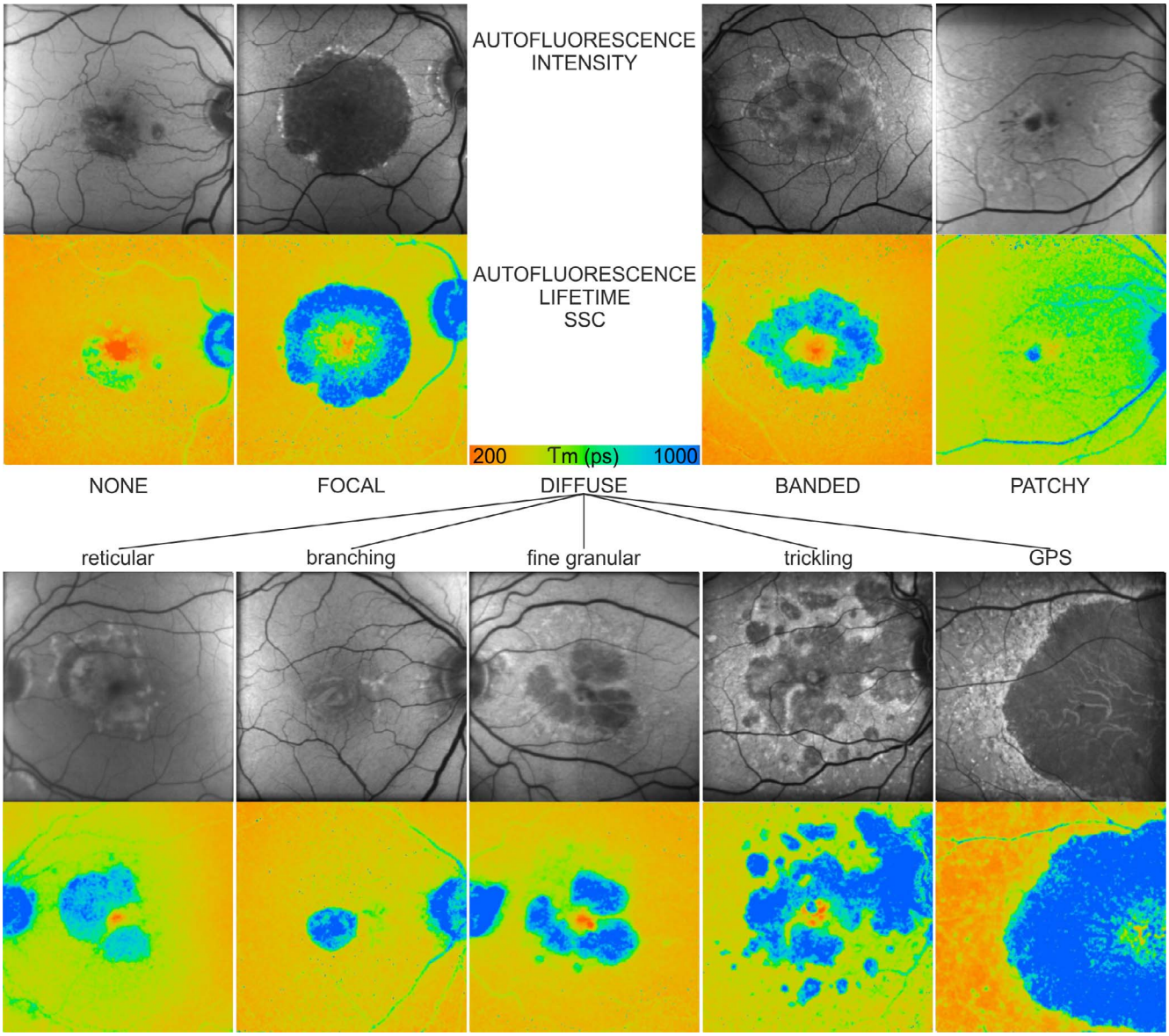

Figure 2. Classification of FAF patterns according to Bindewald et al.[6] Corresponding autofluorescence intensity and mean autofluorescence lifetime images are shown for each subgroup. (*Color scale* always 200–1000 ps). GPS, granular with peripheral punctuate spots.

The mean retinal thickness of the central subfield showed a weak correlation with the BCVA, whereby increased retinal thickness was associated with better ETDRS letter scores ($r^2 = 0.16$, $P = 0.01$). Mean fluorescence lifetimes were independent of the central retinal thickness. Longer lifetimes had a weak but significant association with thicker subfoveal choroidal thickness (SSC: $r^2 = 0.13$, $P = 0.02$; LSC: $r^2 = 0.1$, $P = 0.045$).

Next, we analyzed the seven cases without short autofluorescence lifetimes identifiable within the fovea. In these cases, the OPL was not identifiable in OCT (Figs. 6A, B).

FLIO in GA Borders

In FLIO, the borders of GA were identified to feature mean fluorescence lifetime values shorter than within the main atrophy but longer than the surrounding retina (SSC: 768 ± 43 ps, LSC: 736 ± 20 ps; all $P < 0.0001$). In the autofluorescence intensity images, these intermediate lifetime borders were located within the hypofluorescent area. In areas of hyperfluorescence surrounding the hypofluorescent atrophic areas, only marginally prolonged mean fluorescence lifetimes were measured when compared with the surrounding retina (SSC: 78 ± 12 ps, LSC: 61 ± 8 ps; both P = not significant). Adjacent zones of GA were clearly identifiable in all GA FAF pattern using two-dimensional (2D) analysis (Fig. 8) and phasor analysis (Supplementary Fig. S1).[20]

Analysis of Individual Fluorescence Lifetime Components

Because *Tm* is a function of individual lifetimes ($T1$ and $T2$) and corresponding amplitudes ($\alpha 1$ and $\alpha 2$), we investigated the influence of these components toward the changes seen in *Tm*. Areas outside GA showed a characteristic distribution of the short lifetime component $T1$ versus the long component $T2$, which is depicted in a uniform distribution cloud within the 2D histogram in both spectral channels (Fig. 8). Areas with GA typically showed prolonged lifetime components, especial-

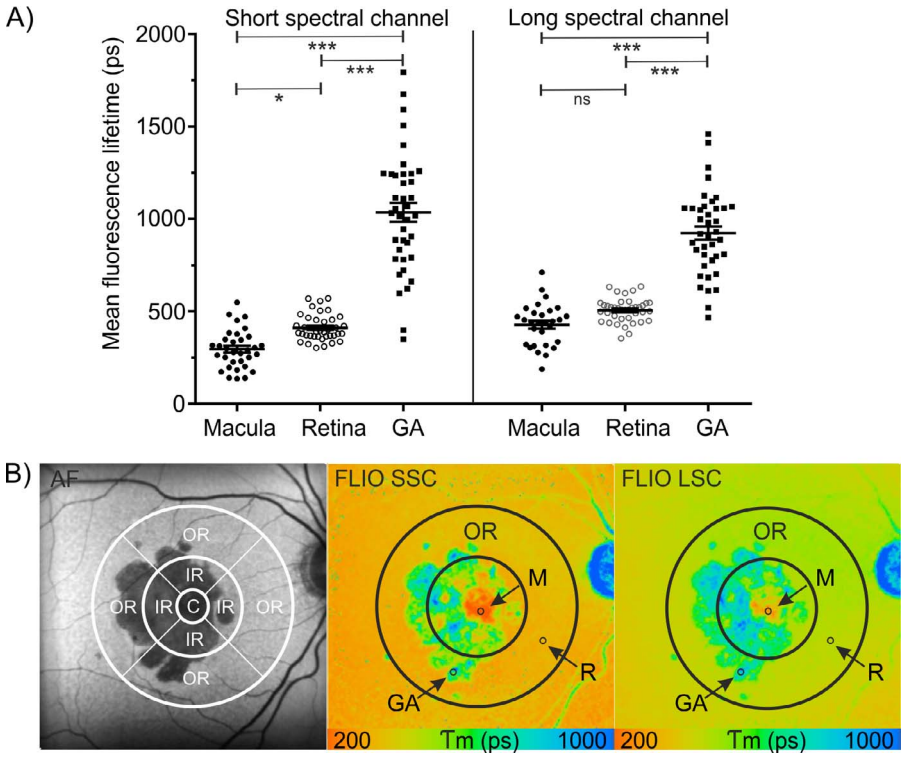

Figure 3. Quantitative analysis of autofluorescence decay times in eyes with dry AMD. (**A**) Mean autofluorescence lifetimes of the macular center, unaffected retina and within areas of GA for both spectral channels (mean ± SEM; $^{*}P < 0.05$, $^{***}P < 0.0001$, $n = 41$). (**B**) For data analysis, a standard ETDRS grid was used (d = 1, 3, and 6 mm). Small areas (circle diameter: 0.2 mm) within the macular center (M) and the OR from unaffected retina (R) and GA were investigated. AF, fundus autofluorescence intensity LSC; C, center; FLIO SSC/LSC, fluorescence lifetime images of the short and the long spectral channels; IR, inner ring; ns, not significant; OR, outer ring.

ly *T*2, resulting in an overall increase of the mean fluorescence lifetime *Tm*. A separate lifetime entity was identified for image pixels located in the adjacent zone of atrophy.

Within GA, the shortest *Tm* values from the macular center resulted from a short *T*1 component with a high amplitude α1, whereby *T*2 was equally distributed within the whole area of GA.

Discussion

Time-resolved autofluorescence lifetime characteristics within areas of GA were investigated in a cohort of 41 patients with dry AMD. Areas of GA featured significantly longer retinal autofluorescence lifetimes when compared with the surrounding retinal tissue. There is a certain degree of variability of absolute FAF lifetimes between different patients because of various factors such as lens status. Because of this, data analysis within individual patients and comparisons of diseased tissue with surrounding unaffected retina was performed.

The adjacent zone bordering on areas of atrophy was clearly identifiable using 2D analysis of fluorescence lifetime values. These diagrams allow for differentiation and visualization of potential tissue at risk for GA known from FAF intensity studies as hyperautofluorescent areas.[21,22] The main fluorescence within the retina originates from lipofuscin, a complex mixture of bisretinoid fluorophores from the visual cycle metabolism.[9,23] According to conventional opinion, hyperfluorescent borders around GA are supposed to contain increased concentrations of lipofuscin.[24] However, in FLIO measurements, corresponding mean fluorescence lifetime values still differ only marginally from values of the surrounding normal retina even though significantly prolonged lifetimes originating from lipofuscin (1262 ps) derivates might be expected.[25,26] Rather, new insights indicate that increased autofluorescence might be caused by vertically superimposed cells and cellular fragments and not by increased lipofuscin concentrations.[12,27] This hypothesis can be supported by our fluorescence lifetime measurements of these areas.

Typically areas of GA show loss of the RPE and the overlaying photoreceptors in OCT. In FLIO, this absence may allow increased contribution of autofluorescence decay times from retinal layers or metabolites with relatively longer lifetimes. They may either originate from the underlying choroid or from within the inner retinal layers. On the other hand, the presence of long lifetimes in patients with GA supports our hypothesis that short decay times mainly come from the RPE. However, in areas of generalized RPE atrophy in FAF and OCT, we found preservation of relatively short autofluorescence lifetimes. A recent study has provided evidence for a strong impact of macular pigment (MP) on macular FAF lifetimes by correlating MP optical density measurements with lifetimes in the fovea.[28] MP consists of the two hydroxycarotenoids, lutein and zeaxanthin, with peak concentrations in the foveal center of the macula.[29] MP is very effective at absorbing short-wavelength blue light with an absorbance peak at 460 nm.[30,31] This can be seen in FAF, where MP is known to decrease an autofluorescence intensity signal, resulting in the typical hypofluorescent macula by absorbing the short-wavelength excitation light. There is little information on the behavior of MP in GA in the literature, presumably because the absence of autofluorescence is masked by the general hypofluorescence caused by GA. Assuming that short lifetimes in the fovea are generated by

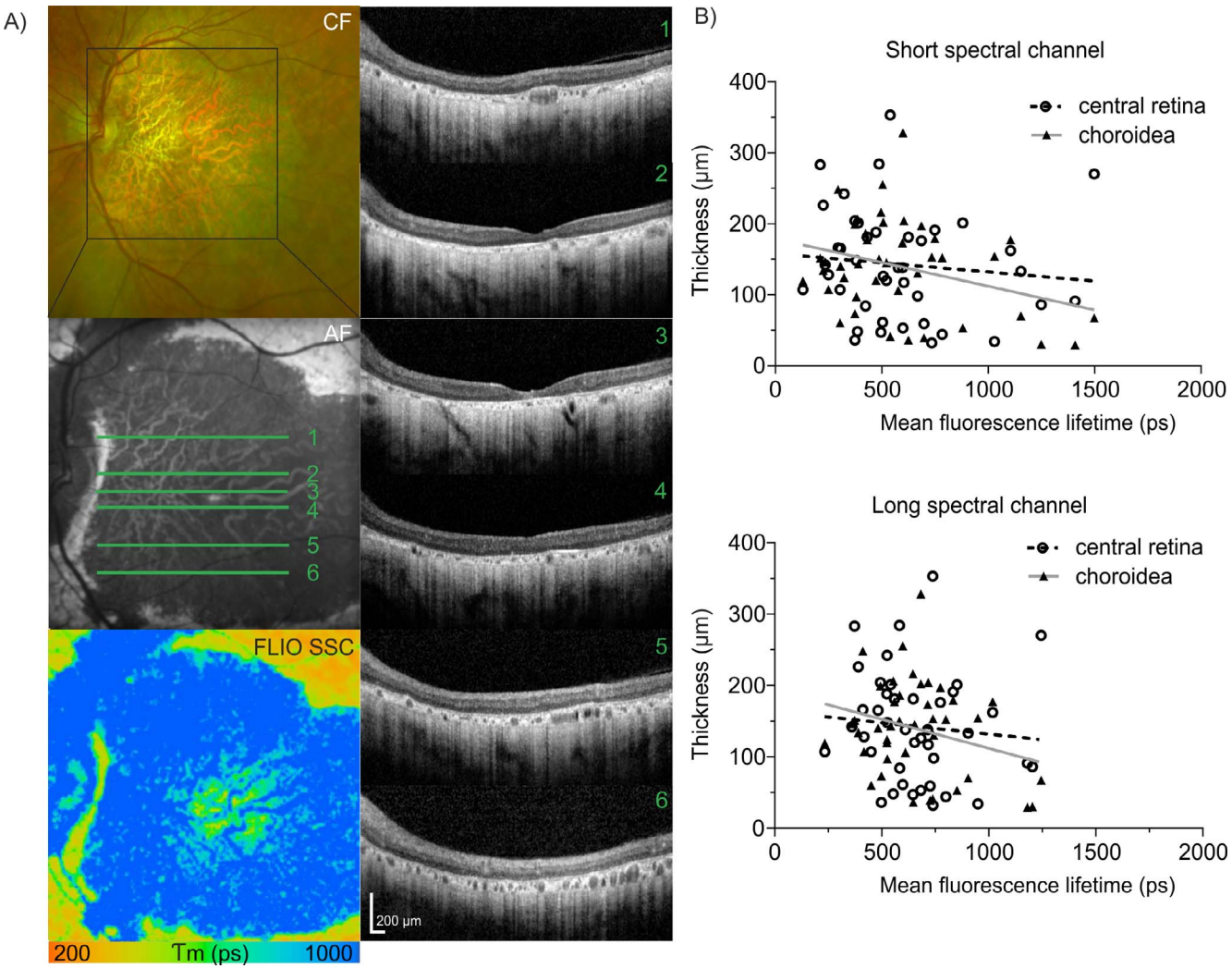

Figure 4. Fluorescence lifetimes within GA. (**A**) FLIO SSC and OCT scans of indicated lines 1 to 6. (**B**) Correlation of mean fluorescence lifetimes of the short (*above*) and long (*below*) spectral channel with central retinal thickness (*dotted line*, not significant) and central choroidal thickness (*gray line*, SSC: $r^2 = 0.13$, $P = 0.02$; LSC: $r^2 = 0.1$, $P = 0.045$). AF, fundus autofluorescence intensity; CF, color fundus.

MP, it is a striking finding that MP is preserved even in the presence of atrophy. Given that MP is mainly found in the plexiform layers and the photoreceptor axon layers, the persistence of MP may reflect the health of the plexiform layers. Interestingly, in some cases the characteristic short lifetimes were absent in the fovea. Correlation with OCT in these cases showed loss of the ONL and OPL within the area of GA. This strongly supports the evidence that short fluorescence lifetimes within the macular center originate from MP. However, given the persistence of short lifetimes even in the presence of central atrophy, short central retinal fluorescence lifetimes alone cannot be used for differentiation of foveal sparing.

In keeping with these findings, long fluorescence lifetimes in patients with central GA were associated with worse visual acuity and thinner subfoveal choroidal thickness. Both findings may point toward an advanced disease stage of GA. These results are in accordance with other studies in which the thinning of the choroid in patients with GA was found[32–34] and even an association with the progression rate was identified.[32] In this late stage, the layer structure of the other retinal layers is mostly destroyed including the Henle fiber layer and the OPL containing the macular pigment.

An advantage of time-resolved autofluorescence is the ability to investigate various lifetime components because *Tm* is a function of individual lifetimes and amplitudes. The individual clustering of pixel values in specific regions can be analyzed using 2D analysis. It is noteworthy that the lifetime cloud of the adjacent zone falls between the surrounding retina and the atrophic zone, which implies that the adjacent zone is influenced by fluorophores that predominate the atrophic area. In this context, a high spatial resolution of FLIO images is important, and therefore the curve-fitting parameters we applied seem to be appropriate.

Our findings of fluorescence lifetime measurement in GA may have an important impact on disease monitoring because they may be an indicator for degenerative processes in the outer retina.

This study shows a broad range of clinical presentations of GA. However, the number of included patients is limited and larger cohorts will have to be analyzed to investigate and evaluate pattern-specific characteristics in the different GA subgroups. Furthermore, additional ex vivo lifetime data will be necessary to dissect the influence of individual components within the border zone of atrophy and the surrounding retina. In addition, longitudinal follow-up examinations and further

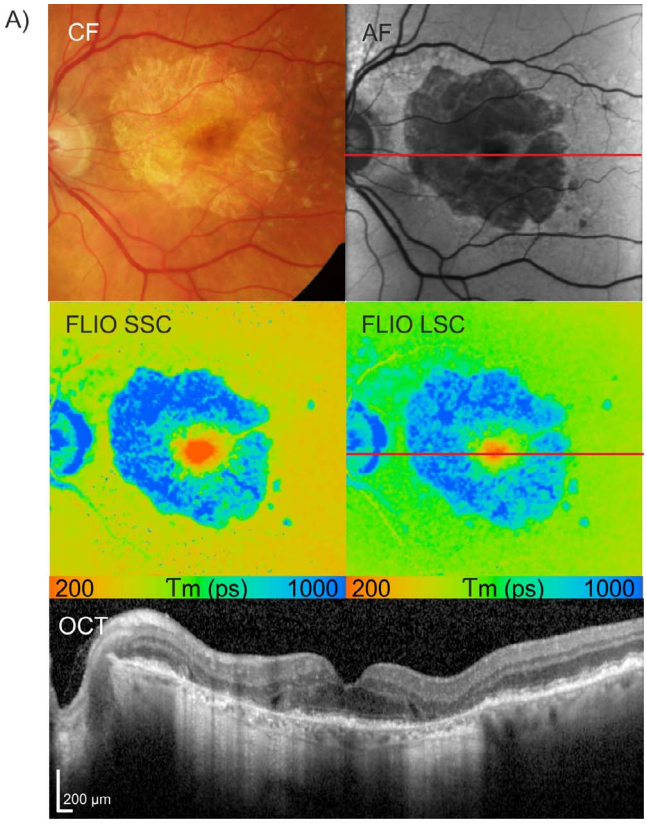

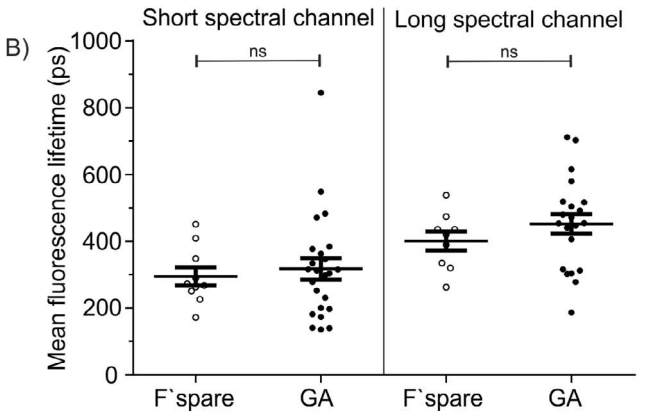

Figure 5. GA with foveal sparing. (**A**) OCT scan of the indicated line. (**B**) Comparison of fluorescence lifetimes within the foveal center in eyes with foveal sparing (F'spare) and central atrophy (GA) ($n = 10$ F'spare; $n = 31$ GA). AF, fundus autofluorescence intensity LSC; CF, color fundus; FLIO SSC/LSC, mean fluorescence lifetime images of the short and the long spectral channels; ns, not significant.

correlation with functional parameters are needed to identify markers for disease progression.

Conclusions

Fluorescence lifetime analysis of areas with GA provides specific lifetime patterns. Short fluorescence lifetimes within the macular center may provide information about the integrity of the OPL and ONL. The analysis of GA borders by FLIO might emerge as a useful tool for the visualization of local tissue remodeling and disease monitoring.

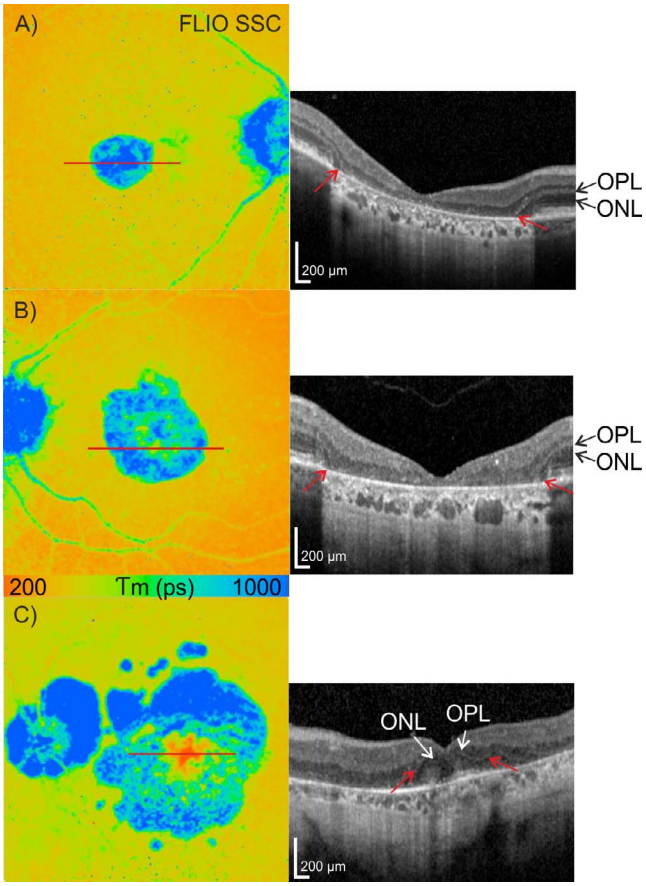

Figure 6. FLIO (SSC) and OCT in GA without short central autofluorescence lifetimes. (**A, B**) The ONL and the OPL are completely missing within the area of GA. (**C**) Example with preserved ONL and OPL and short mean autofluorescence lifetimes within the foveal center.

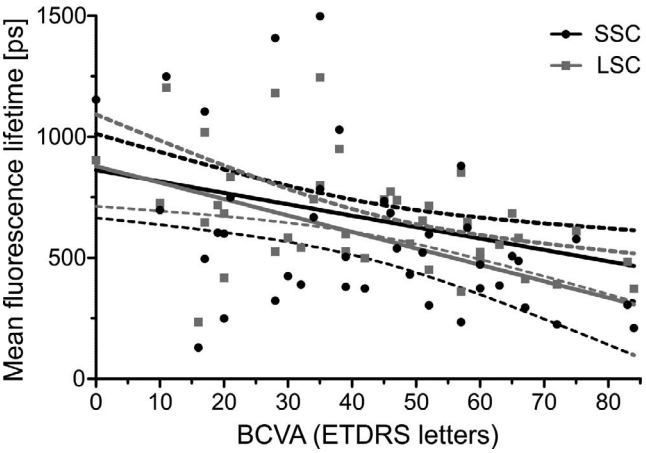

Figure 7. Correlation of mean fluorescence lifetime values with best corrected visual acuity (BCVA, ETDRS letters). Mean values from the central subfield with *error bars* (95%, *dotted lines*) are shown for the short and the long spectral channels (both $r^2 = 0.19$, $P = 0.004$). SSC = *black*; LSC = *gray*.

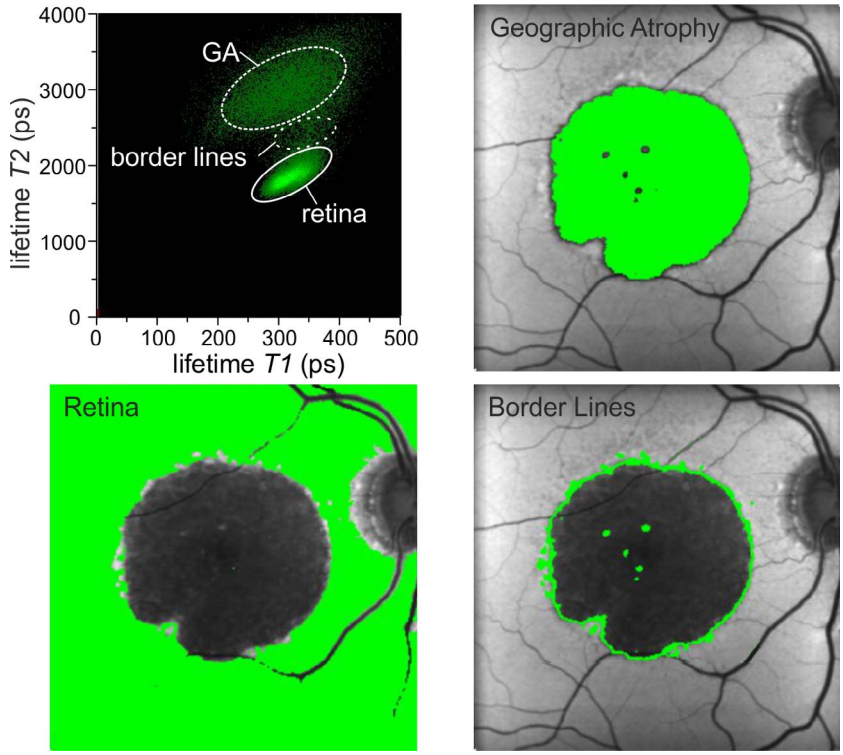

Figure 8. Distribution of fluorescence lifetime components in GA. Distribution histogram of the short decay component *T*1 versus the long decay component *T*2 (see also Equation 1). Specific lifetime distribution clusters were identified for the unaffected retina, GA, and the adjacent zone of GA.

Acknowledgments

The authors thank Jörg Fischer, PhD, Yoshihiko Katayama, PhD, and Kester Nahen, PhD, from Heidelberg Engineering GmBH (Heidelberg, Germany), for providing technical assistance for the FLIO device.

Supported by a grant from the Swiss National Science Foundation (320030_156019; Bern, Switzerland).

Disclosure: **C. Dysli**, Heidelberg Engineering (S); **S. Wolf**, Heidelberg Engineering (C, S), Bayer (C), Novartis, (C), Alcon (C), Allergan (C), Roche (C); **M.S. Zinkernagel**, Heidelberg Engineering (S), Bayer (C), Novartis (C, I)

References

1. McHarg S, Clark SJ, Day AJ, Bishop PN. Age-related macular degeneration and the role of the complement system. *Mol Immunol*. 2015;67:43–50.
2. Resnikoff S, Pascolini D, Etya'ale D, et al. Global data on visual impairment in the year 2002. *Bull World Health Organ*. 2004; 82:844–851.
3. Clemons TE, Milton RC, Klein R, Seddon JM, Ferris FL III; Age-Related Eye Disease Study Research Group. Risk factors for the incidence of Advanced Age-Related Macular Degeneration in the Age-Related Eye Disease Study (AREDS) AREDS report no. 19. *Ophthalmology*. 2005;112:533–539.
4. Klein RJ, Zeiss C, Chew EY, et al. Complement factor H polymorphism in age-related macular degeneration. *Science*. 2005;308:385–389.
5. Maller J, George S, Purcell S, et al. Common variation in three genes, including a noncoding variant in CFH, strongly influences risk of age-related macular degeneration. *Nat Genet*. 2006;38:1055–1059.
6. Bindewald A, Bird AC, Dandekar SS, et al. Classification of fundus autofluorescence patterns in early age-related macular disease. *Invest Ophthalmol Vis Sci*. 2005;46:3309–3314.
7. Schmitz-Valckenberg S, Fleckenstein M, Gobel AP, et al. Evaluation of autofluorescence imaging with the scanning laser ophthalmoscope and the fundus camera in age-related geographic atrophy. *Am J Ophthalmol*. 2008;146:183–192.
8. Holz FG, Bindewald-Wittich A, Fleckenstein M, et al. Progression of geographic atrophy and impact of fundus autofluorescence patterns in age-related macular degeneration. *Am J Ophthalmol*. 2007;143:463–472.
9. Delori FC, Dorey CK, Staurenghi G, Arend O, Goger DG, Weiter JJ. In vivo fluorescence of the ocular fundus exhibits retinal pigment epithelium lipofuscin characteristics. *Invest Ophthalmol Vis Sci*. 1995;36:718–729.
10. Sparrow JR, Fishkin N, Zhou J, et al. A2E, a byproduct of the visual cycle. *Vis Res*. 2003;43:2983–2990.
11. Ach T, Huisingh C, McGwin G Jr, et al. Quantitative autofluorescence and cell density maps of the human retinal pigment epithelium. *Invest Ophthalmol Vis Sci*. 2014;55: 4832–4841.
12. Rudolf M, Vogt SD, Curcio CA, et al. Histologic basis of variations in retinal pigment epithelium autofluorescence in eyes with geographic atrophy. *Ophthalmology*. 2013;120:821–828.
13. Sparrow JR, Yoon KD, Wu Y, Yamamoto K. Interpretations of fundus autofluorescence from studies of the bisretinoids of the retina. *Invest Ophthalmol Vis Sci*. 2010;51:4351–4357.
14. Sayegh RG, Simader C, Scheschy U, et al. A systematic comparison of spectral-domain optical coherence tomography and fundus autofluorescence in patients with geographic atrophy. *Ophthalmology*. 2011;118:1844–1851.
15. Dysli C, Quellec G, Abegg M, et al. Quantitative analysis of fluorescence lifetime measurements of the macula using the fluorescence lifetime imaging ophthalmoscope in healthy subjects. *Invest Ophthalmol Vis Sci*. 2014;55:2106–2113.

16. Dysli C, Wolf S, Zinkernagel MS. Fluorescence lifetime imaging in retinal artery occlusion. *Invest Ophthalmol Vis Sci*. 2015; 56:3329–3336.
17. Schweitzer D, Hammer M, Schweitzer F, et al. In vivo measurement of time-resolved autofluorescence at the human fundus. *J Biomed Opt*. 2004;9:1214–1222.
18. Schweitzer D, Schenke S, Hammer M, et al. Towards metabolic mapping of the human retina. *Microsc Res Tech*. 2007;70:410–419.
19. Early Treatment Diabetic Retinopathy Study Research Group. Early treatment diabetic retinopathy study design and baseline patient characteristics. ETDRS report number 7. *Ophthalmology*. 1991;98(suppl):741–756.
20. Digman MA, Caiolfa VR, Zamai M, Gratton E. The phasor approach to fluorescence lifetime imaging analysis. *Biophys J*. 2008;94:L14–L16.
21. Bearelly S, Khanifar AA, Lederer DE, et al. Use of fundus autofluorescence images to predict geographic atrophy progression. *Retina*. 2011;31:81–86.
22. Bindewald A, Schmitz-Valckenberg S, Jorzik JJ, et al. Classification of abnormal fundus autofluorescence patterns in the junctional zone of geographic atrophy in patients with age related macular degeneration. *B J Ophthalmol*. 2005;89:874–878.
23. Sparrow JR, Duncker T. Fundus autofluorescence and rpe lipofuscin in age-related macular degeneration. *J Clin Med*. 2014;3:1302–1321.
24. Holz FG, Steinberg JS, Gobel A, Fleckenstein M, Schmitz-Valckenberg S. Fundus autofluorescence imaging in dry AMD: 2014 Jules Gonin lecture of the Retina Research Foundation. *Graefe's Arch Clin Exp Ophthalmol*. 2015;253:7–16.
25. Schweitzer D. Metabolic mapping. In: Holz FG, Spaide RF, eds. *Medical Retina (Essentials in Ophthalmology)*. Berlin, Germany: Springer; 2010:107–123.
26. Schweitzer D, Gaillard ER, Dillon J, et al. Time-resolved autofluorescence imaging of human donor retina tissue from donors with significant extramacular drusen. *Invest Ophthalmol Vis Sci*. 2012;53:3376–3386.
27. Holz FG, Strauss EC, Schmitz-Valckenberg S, van Lookeren Campagne M. Geographic atrophy: clinical features and potential therapeutic approaches. *Ophthalmology*. 2014;121: 1079–1091.
28. Sauer L, Schweitzer D, Ramm L, Augsten R, Hammer M, Peters S. Impact of macular pigment on fundus autofluorescence lifetimes. *Invest Ophthalmol Vis Sci*. 2015;56:4668–4679.
29. Bone RA, Landrum JT, Tarsis SL. Preliminary identification of the human macular pigment. *Vis Res*. 1985;25:1531–1535.
30. Snodderly DM, Brown PK, Delori FC, Auran JD. The macular pigment. I. Absorbance spectra, localization, and discrimination from other yellow pigments in primate retinas. *Invest Ophthalmol Vis Sci*. 1984;25:660–673.
31. Trieschmann M, Heimes B, Hense HW, Pauleikhoff D. Macular pigment optical density measurement in autofluorescence imaging: comparison of one- and two-wavelength methods. *Graefe's Arch Clin Exp Ophthalmol*. 2006;244:1565–1574.
32. Lee JY, Lee DH, Lee JY, Yoon YH. Correlation between subfoveal choroidal thickness and the severity or progression of nonexudative age-related macular degeneration. *Invest Ophthalmol Vis Sci*. 2013;54:7812–7818.
33. Lindner M, Bezatis A, Czauderna J, et al. Choroidal thickness in geographic atrophy secondary to age-related macular degeneration. *Invest Ophthalmol Vis Sci*. 2015;56:875–882.
34. Adhi M, Lau M, Liang MC, Waheed NK, Duker JS. Analysis of the thickness and vascular layers of the choroid in eyes with geographic atrophy using spectral-domain optical coherence tomography. *Retina*. 2014;34:306–312.

Investigative Ophthalmology & Visual Science